Environmental Toxicology and Chemistry—Volume 00, Number 00—pp. 1–14, 2021
Received: 31 March 2021 | Revised: 10 May 2021 | Accepted: 7 August 2021

Environmental Toxicology

Temporal Variability of Microparticles Under the Seattle Aquarium, Washington State: Documenting the Global Covid-19 Pandemic

Lyda S.T. Harris,[a,*] Laura La Beur,[a] Amy Y. Olsen,[a] Angela Smith,[a] Lindsey Eggers,[a] Emily Pedersen,[b] Jennifer Van Brocklin,[b] Susanne M. Brander,[b] and Shawn Larson[a]

[a]Seattle Aquarium, Seattle, Washington, USA
[b]Oregon State University, Corvallis, Oregon, USA

Abstract: Anthropogenic debris including microparticles (<5 mm) are ubiquitous in marine environments. The Salish Sea experiences seasonal fluctuations in precipitation, river discharge, sewage overflow events, and tourism—all variables previously thought to have an impact on microparticle transport and concentrations. Our goals are two-fold: 1) describe long-term microparticle contamination data including concentration, type, and size; and 2) determine if seasonal microparticle concentrations are dependent on environmental or tourism variables in Elliott Bay, Salish Sea. We sampled 100 L of seawater at a depth of approximately 9 m at the Seattle Aquarium, Seattle, Washington State, United States, approximately every two weeks from 2019 through 2020 and used an oil extraction protocol to separate microparticles. We found that microparticle concentrations ranged from 0 to 0.64 particles L^{-1} and fibers were the most common type observed. Microparticle concentrations exhibited a breakpoint on 10 April 2020, where estimated slope and associated microparticle concentration significantly declined. Further, when considering both environmental as well as tourism variables, temporal microparticle concentration was best described by a mixed-effects model, with tourism as the fixed effect and the person counting microparticles as the random effect. Although monitoring efforts presented set out to identify effects of seasonality and interannual differences in microparticle concentrations, it instead captured an effect of decreased tourism due to the global Covid-19 pandemic. Long-term monitoring is critical to establish temporal microparticle concentrations and to help researchers understand if there are certain events, both seasonal and sporadic (e.g., rain events, tourism, or global pandemics), when the marine environment is more at risk from anthropogenic pollution. *Environ Toxicol Chem* 2021;00:1–14.

Keywords: Microplastic; Pollution; Puget Sound; Microfiber; Contamination

INTRODUCTION

Anthropogenic debris including microparticles and microplastics (plastic 1 μm–5 mm; Arthur et al., 2009; Hartmann et al., 2019) are ubiquitous in marine environments around the globe (Barrows et al., 2018; Law, 2017). The field of marine microparticles and microplastics is relatively new (e.g., the term "microscopic plastic" was first noted in Thompson et al., 2004) and has grown exponentially over the past decade (Barboza & Gimenez, 2015; Harris, 2020). Due to the rapid growth of the field and advancement in methodology, many previous studies describe all particles found as "microplastics" when polymer analyses have not been done. Therefore, there are disparities in the literature on what types (polymer composition) of particles have been found in marine environments and discrepancies when comparing studies by different authors across organisms or environments (Hartmann et al., 2019). In the present study, we define microparticles (1 μm–5 mm) as a single umbrella term to encompass all suspected micro anthropogenic debris and use microplastics to indicate positive identification through polymer analysis.

Microparticles have been found in surface, pelagic, and deep waters (Davis & Murphy, 2015; Galgani et al., 2015; Choy et al., 2019), coastal and subtidal sediments (Browne

This article includes online-only Supporting Information.

* Address correspondence to lydaharris@gmail.com.
Published online 11 August 2021 in Wiley Online Library (wileyonlinelibrary.com).
DOI: 10.1002/etc.5190

et al., 2011; Pagter et al., 2020), and organisms of multiple functional groups and trophic levels (e.g., filter feeders, deposit feeders, and omnivores; Lusher et al., 2014; Li et al., 2015; Zhang et al., 2021). Whereas researchers do not fully understand the impacts microparticles may have on marine ecosystems, there is growing evidence that they have negative impacts on marine organisms in each of the aforementioned functional groups (e.g., Wright et al., 2013; Galloway et al., 2017; Harris and Carrington, 2019; Harris et al., 2021).

Marine environments are dynamic and fluctuate from season to season and year to year because waters are continually changing with the tides, currents, and fluvial inputs (e.g., Uncles et al., 2000). Large-scale mechanisms driving global, spatial transportation and accumulation of marine microparticles may include currents and Ekman convergent basins (a result of the net motion between Coriolis and wind forces; Barnes et al., 2009; van Sebille et al., 2020), whereas small-scale mechanisms include region-specific bathymetry and environmental factors (Critchell & Lambrechts, 2016). For example, a positive correlation between rainfall and accumulation of plastic debris has been observed on beaches (Ivar do Sul & Costa, 2014; Cheung et al., 2016) and in estuaries (Lima et al., 2014).

The Salish Sea, bordered by Washington State, the United States, and British Columbia, Canada, is an ideal region to study microparticle contamination due to its concentrated urban environments, history of industrialization, seasonal precipitation, and region-specific bathymetry and environmental factors. The Salish Sea is characterized as a large and deep estuary consisting of smaller regional basins; it has sizable fresh and saltwater inputs year-round, and is home to charismatic megafauna (e.g., sea otters and orcas) and economically important species (e.g., salmon, mussels, rockfish, and oysters). The Salish Sea is also subjected to effluents of large coastal cities such as Seattle and Tacoma in the state of Washington, and Victoria and Vancouver in British Columbia. This juxtaposition of ecologically and economically valuable ecosystems with sizable adjacent urban populations makes the Salish Sea an ideal location to study regional and temporal marine microparticle contamination levels.

The primary factors influencing regional spatial transportation and accumulation of marine microparticles in locations resembling the Salish Sea are wind direction and strength, quantity of rainfall, surface runoff, rivers, and storm water drainage during wet seasons (Browne et al., 2010; Critchell & Lambrechts, 2016; Zhang, 2017; Wichmann et al., 2019). The same small-scale mechanisms may drive spatial transportation and accumulation of microparticles in the Salish Sea region (Gilman, 2013; Hansen, 2016). The region receives high rainfall for much of the winter, and the quantity of urban runoff and wastewater effluent increases. Rising spring temperatures cause snowmelt from nearby mountain ranges (Cascade and Olympic Mountains) to increase river levels, and more microparticles are carried as water makes its way to the Salish Sea (Van Emmerik et al., 2019). In addition, changing surface temperatures cause seawater turnover events that mix layers and disrupt stratification. Mixing may lead to microparticle transport that disrupts perceived annual patterns and may go undetected if sample collection only occurs sporadically. In summer, the region experiences little rainfall and snowmelt but rather elevated temperatures that lead to evaporation and strong thermal and salinity stratification. These seasonal changes are accompanied by fluctuations in urban populations and tourism, boat traffic, and marine animal migrations.

Previous studies point toward seasonality as a key indicator of microparticle concentrations (e.g., Van Emmerik et al., 2019) and increase the need for regular and long-term monitoring to understand how contamination changes temporally in regions with wet and dry seasons. Most environmental microparticle contamination studies, especially in the Salish Sea, focus on geographic rather than temporal differences (Pacific Northwest Microplastics Workshop, 2021). Microparticle pollution in the Salish Sea is likely generated from adjacent cities, populations, and industries (Desforges et al., 2014; Davis & Murphy, 2015), and is distributed by winds, currents, tides, and geomorphic processes (Desforges et al., 2014; Davis & Murphy, 2015; Hofmans, 2017; Mahoney, 2017; Serdan, 2017). The predominant microparticle morphotypes found in surface water tows in the region are foam (Davis & Murphy, 2015) and fibers (Desforges et al., 2014). The latter is reflected in microparticles found in oysters, albeit in low quantities (Martinelli et al., 2020), and in razor clams from the outer Washington coast (Baechler et al., 2020). Unpublished data from undergraduate student theses and capstone projects (a capstone project is a multifaceted body of work that serves as a culminating academic and intellectual experience for students) indicate that microparticle abundance is greater at depth than at the surface in the Salish Sea (Hansen, 2016; Moats, 2019). These findings are supported by peer-reviewed literature from other regions that found levels of microparticles are highest in mid-pelagic waters (Enders et al., 2015; Choy et al., 2019).

Unfortunately, critical baseline concentrations and seasonality shifts remain unknown, hindering the ability to determine how local species, including humans, are impacted by shifts in microparticle loads. It is critical to measure long-term microparticle concentrations to establish a temporal baseline, document anthropogenic anomalies, and help researchers understand if there are certain times (e.g., seasonal rains, combined sewage overflows, tourist seasons, etc.) when the Salish Sea is more at risk from microparticle influx. A temporal understanding will provide information to policymakers and resource managers to better support and protect this ecologically rich and economically important region.

The Seattle Aquarium is located at Pier 59 on the Elliott Bay waterfront in the central Puget Sound region of the southern Salish Sea. The Aquarium draws seawater at depth directly from Elliott Bay for exhibits, and provides an ideal location for long-term water monitoring. Initially, the Seattle Aquarium set out to establish baseline microparticle concentrations and seasonality in Elliott Bay through ongoing water column sampling. The duration (2019–2020) of the present study occurred before and during the global Covid-19 pandemic with associated reductions in human activity, which presented an unprecedented opportunity to capture pre-pandemic and mid-pandemic contamination baselines. Due to the Aquarium's unique location,

the composition of our research team, and ongoing monitoring efforts, the present study provides the first long-term microparticle monitoring results of microparticle concentrations in the Salish Sea. Our goals are two-fold: 1) describe long-term microparticle contamination data including concentration, particle type, and particle size; and 2) determine if seasonal microparticle concentrations are dependent on environmental or tourism variables in Elliott Bay, Salish Sea.

MATERIALS AND METHODS

The Seattle Aquarium, a nonprofit and nongovernment organization, operates a small research team through the Conservation Programs and Partnerships Department. The microplastics research laboratory and team are unique in that research focuses on volunteer efforts and community engagement while still carrying out rigorous protocols. The marine microplastic team is composed of permanent and temporary staff as well as volunteers. To ensure the use of the most up-to-date methods, the Aquarium's research capacity, and composition of volunteers and staff, collection and processing protocols were changed during the present study. A timeline of changes is described in Table 1.

Water collection

Seawater samples were collected at the Seattle Aquarium (47°36'26.6"N, 122°20'38.3"W). The water collection procedure described was adopted from methods used by, and communications with, the Ocean Wise plastics research team in Vancouver, Canada. Water samples were collected approximately once per month from January through July 2019 and approximately every 2 weeks (bi-monthly) from August 2019 through December 2020 (some collection dates were missed due to staff and volunteer availability). Seawater was drawn directly from Elliott Bay into the Aquarium via a pump located approximately 9 m below the Aquarium pier (depth of water fluctuated with tidal changes; tides ranged from −1.04 m to +4.01 m during the present study; National Oceanic and Atmospheric Administration [NOAA] tide predictions). To capture anthropogenic microparticles, 100 L of seawater was siphoned from the pumps and passed through either a 10 inch diameter (January 2019–December 2019) or a 3 inch diameter (January 2020–December 2020) covered 63-μm mesh, stainless steel sieve (Desforges et al., 2014; Crichton et al., 2017). The covered sieve was transported to a clean room (January 2019–March 2020) or laminar-flow hood (April 2020–December 2020) to either undergo immediate processing or be rinsed into acid-washed glassware with ultrapure deionized water, covered with aluminum foil, and stored in a refrigerator (~5 °C) until processed.

Microplastic extraction

Samples underwent an oil extraction protocol to separate microparticles from biotic material (Crichton et al., 2017). Captured particles in the 10 inch sieve were rinsed into a metal collection pan with deionized water and then into a glass separatory funnel, while captured particles in the 3 inch sieve were rinsed directly into a glass separatory funnel with deionized water via a glass funnel. Stored samples were poured directly into the glass separatory funnel and the storage glassware rinsed with deionized water. Canola oil from a glass bottle was added to the separatory funnel, using 5 ml of oil for every 100 ml of deionized water. The separatory funnel was gently shaken, and the mixture was allowed to settle for 2 min until distinct layers formed. The bottom layer was discarded, and the remaining oil layer was vacuum filtered through 0.45 μm of mixed cellulose ester filter paper (Advantec; 47 mm). The separatory funnel was rinsed twice with 25 ml of diluted detergent (1% Liquinox Critical-Cleaning Liquid Detergent; Alconox) and deionized water and subsequently filtered to ensure all microparticles were captured. The filter paper was incubated twice in 10 ml of 95% ethanol for 10 min to clean particles of any oil residue that might interfere with spectroscopy. After ethanol washing, filter papers were transferred to a plastic Petri slide (Millipore SAS) using metal fan tweezers and immediately covered with a lid.

Visualization and quantification

Filters were visually inspected under a microscope (Olympus SZX10 stereoscope) with a camera attachment (Olympus SC50). Microparticles were categorized by morphotype and color, then measured using cellSens software (length or area; OLYMPUS cellSens Entry 2.3). Only microparticles 330 to 5000 μm (length; Masura et al., 2015) were categorized and measured due to the resolution of the microscope and camera.

During visual inspection, it is nearly impossible to determine polymer composition; therefore, all particles that appeared to be of anthropogenic origin were counted and categorized by morphotype and color (Figure 1). Morphotypes included fibers, foils, and fragments. Particle color was recorded as the primary color found on the majority of the particle (some particles had multiple colors but only one color was recorded for the purpose of analyses). Rare colors (<1% of total observations) were recorded and categorized as "other" for analyses.

TABLE 1: Dates and changes in sampling methodology, equipment, and processing locations at the Seattle Aquarium (2019–2020)

Date	Method
1/1/2019	Collected water approximately once per month 10 inch sieve Sieve was DIW-rinsed and covered with aluminum foil MP rinsed from sieve into pan, and pan was rinsed into separatory funnel OEP in clean room
1/8/2019	Collected water approximately twice per month
1/1/2020	3 inch sieve Sieve was cleaned in sonicator and covered with aluminum foil MP rinsed from sieve into separatory funnel
27/3/2020	Moved from clean room and began OEP in laminar-flow hood in the laboratory

DIW = deionized water; MP = microparticles; OEP = oil extraction protocol.

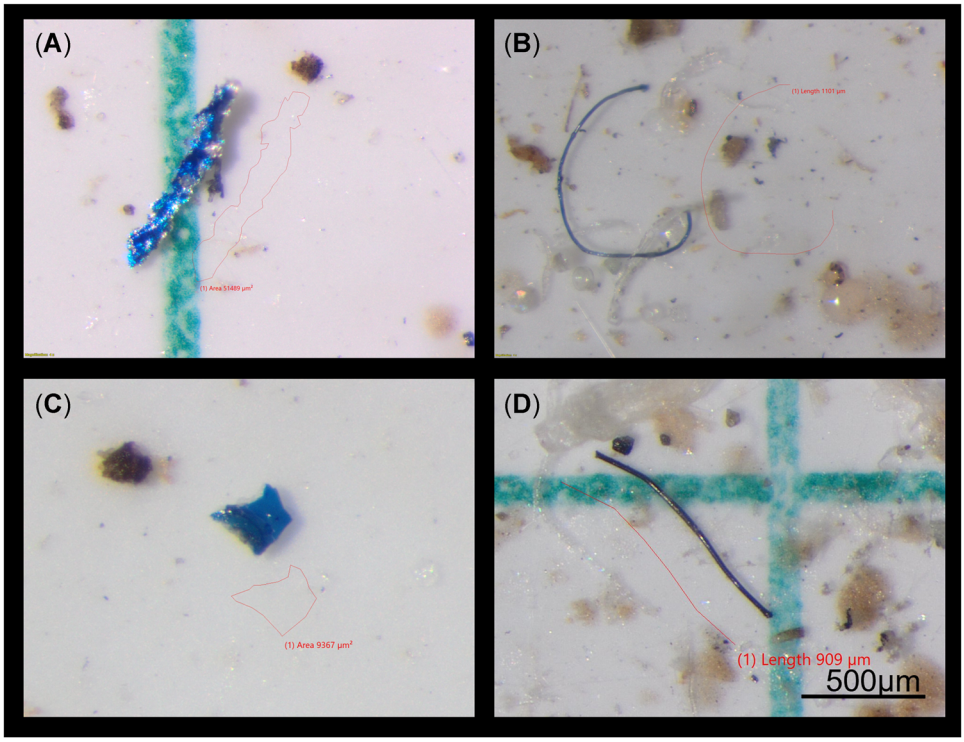

FIGURE 1: Examples of different morphologies and colors. Photos are representative samples of (**A**) Blue foil. (**B**) Blue fiber. (**C**) Blue fragment. (**D**) Black fiber.

Polymer analysis

Approximately 10% (76 of 726 total particles) of suspected anthropogenic microparticles were picked from sample filters for micro-Fourier transform infrared (µFTIR) spectroscopy analysis (Thermo Electron iN5 µFTIR; Thermo Fisher Scientific). A subset of filters was shipped from the Seattle Aquarium to Oregon State University for µFTIR analysis. Within the subset of filters, chosen microparticles were representative of the quantities found over time, sample types (water and blanks), colors, and morphologies of particles observed. Subsampling was performed visually with a Leica EZ4 microscope and Motic 3+ camera. Under a laminar-flow hood, subsampled microparticles were picked from filters, stored on glass microscope slides, and secured with a glass coverslip and tape. Samples were first visualized on slides using a dissecting scope (Leica EZ4 E) to get a matching length measurement and positive ID by comparing them with visual and length data recorded at the time of picking from filters. Samples were then placed on a gold-plated slide in a drop of 70% filtered ethanol to prevent movement during transport to the µFTIR. The slide was placed on the stage of the µFTIR and ethanol was allowed to evaporate before analysis. Reflectance was measured using a fixed aperture with 128 to 512 scans on the largest, cleanest portion of the sample. A germanium tip probe was inserted and lowered to contact the sample (~1–2 µm into material surface) for further spectral analysis. A math match of 70 or greater using either or both overall reflectance and attenuated reflectance (µATR) is the standard during sample analysis. The sample was then retrieved, when possible (sometimes samples stuck to or broke on contact with an µATR tip), after data collection and returned to its respective slide. Polymer identifications from Open Specy, open-source software that performs baseline correction and smoothing, as well as matches with microplastic-specific databases (Cowger et al., 2021), were used due to higher matching percentages; however, polymer identifications were cross-checked with identifications from Omnic (Thermo Fisher Scientific software) to confirm microparticle categorizations.

Quality assurance/quality control

To reduce airborne and ambient anthropogenic microparticle contamination, all equipment underwent extensive cleaning before sampling and oil extraction protocol. The 10 inch metal sieve was triple rinsed, and the 3 inch metal sieve was cleaned in a sonic cleaner (Cole-Palmer Ultrasonic Cleaner; Model 08895-04); all sieves were covered with aluminum foil before and during each sampling event. All glassware received an acid rinse and deionized water rinses (total of three) before May 2019; beginning in late May 2019, all glassware was soaked in an acid bath and rinsed thoroughly with deionized water. All glassware was then covered with aluminum foil before and during use. Samples collected before April 2020 were processed and filtered in a clean room, whereas samples collected in April 2020 and onward were processed and filtered in a laminar-flow hood (Security Air Systems). After oil extraction protocol, filters were placed in plastic Petri slides, where the lids remained on throughout drying and visual quantification. Researchers wore white 100% cotton laboratory coats and latex gloves during collection, processing, and polymer analyses.

A blank filter paper in an open Petri slide was placed in the necropsy room and a laminar-flow hood was used during sample processing to collect ambient air microparticles.

Environmental and tourism data

Environmental and tourism data used in model selection were acquired from open-access sources. Precipitation data (mm day^{-1}) were collected from the Seattle-Tacoma International Airport station (47°26'56.3"N, 122°18'28.8"W) 1 January 2019 through 1 January 2021 (National Centers of Environmental Information at NOAA; Figure 2A). Duwamish River discharge ($m^3\ day^{-1}$) data were collected from the Tukwila, Washington, golf courses (47°29'01.8"N, 122°15'36.6"W) 1 January 2019 through 1 January 2021 (US Geological Survey Water Resources; Figure 2B). Wastewater effluent included data from wastewater treatment plants (WWTP; West Point and South Plant), combined sewer overflow treatment facilities (Alki, MLK, Elliott West, and Carkeek), and untreated combined sewer overflow facilities (numerous; million $m^3\ day^{-1}$) in Puget Sound were collected from the King County Wastewater Treatment Division on request 1 January 2019 through 1 January 2021 (Figure 2C). To capture a metric for general tourism trends, individuals traveling through Transportation Security Administration (TSA) screened areas at Seattle-Tacoma International Airport (people day^{-1}) were used as a proxy and collected from the Port of Seattle 1 January 2019 through 1 January 2021 (Figure 2D). While the quantity of people traveling via air does not capture all human activity in Seattle (car, train, etc.), and may have been disproportionately affected by Covid-19, data from individuals passing through TSA screened areas provide an open-access metric to measure human movement over time (cruise ship travel was not considered because a no-sail order by the Centers for Disease Control and Prevention occurred on 4 March 2020). Further, global air and road traffic decreased 75 and 50%, respectively, and the percentage of Seattle's population actively in transit fell drastically upon the onset and progression of the pandemic

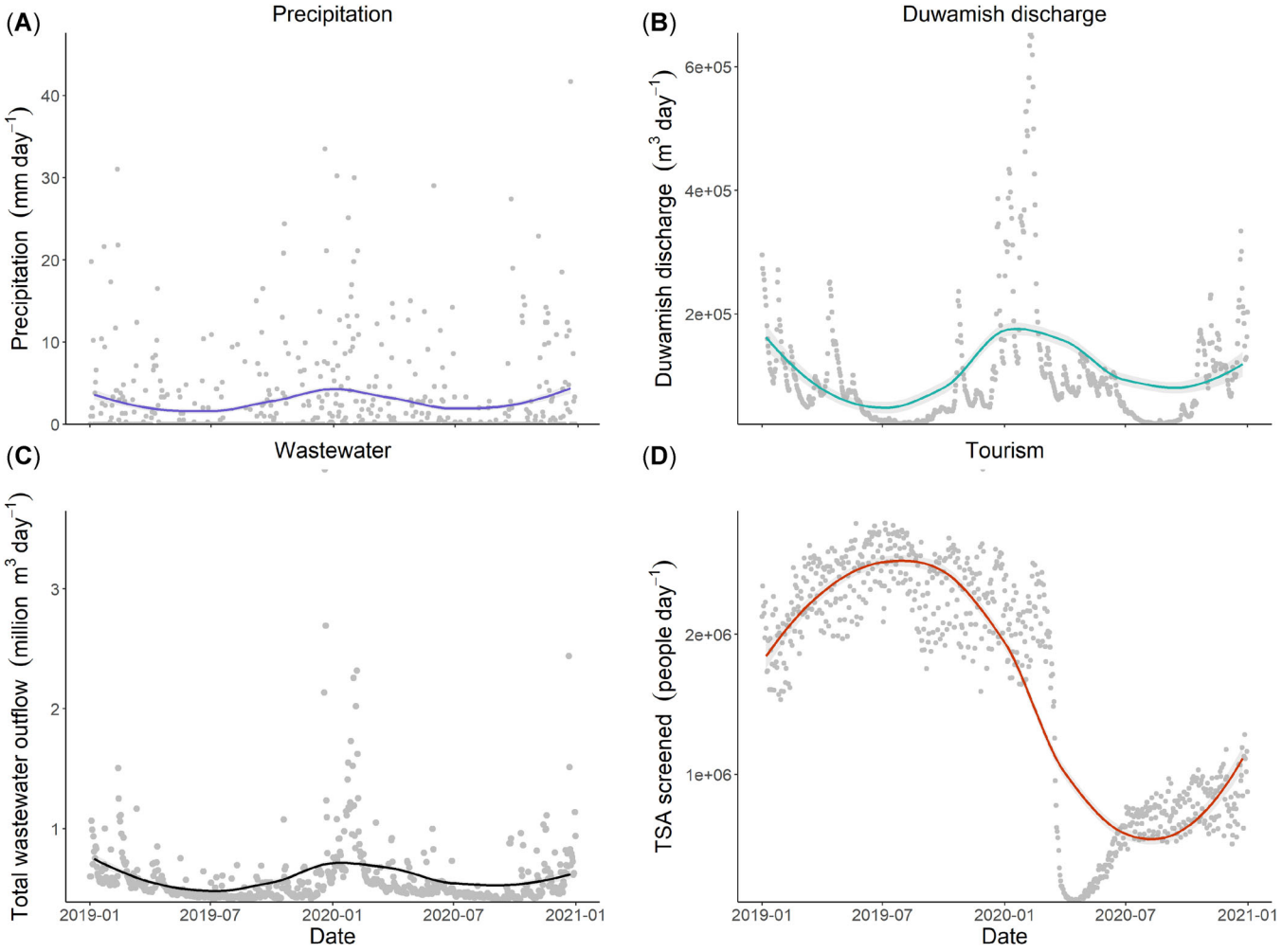

FIGURE 2: Environmental and tourism data used for model selection. Variables include the following. (**A**) Precipitation (mm day^{-1}) accumulation at Seattle-Tacoma International Airport. (**B**) Duwamish River tidal discharge ($m^3\ day^{-1}$) at Tukwila Golf Course. (**C**) Total wastewater effluent (million $m^3\ day^{-1}$) released into Elliott Bay and Puget Sound (wastewater treatment plants, treated combined sewage overflow, and untreated combined sewage overflow). (**D**) Total individuals screened by the Transportation Security Administration (TSA) at Seattle-Tacoma International Airport as a proxy for tourism (people day^{-1}). Gray dots denote daily measurements and colored lines represent 14-day rolling averages.

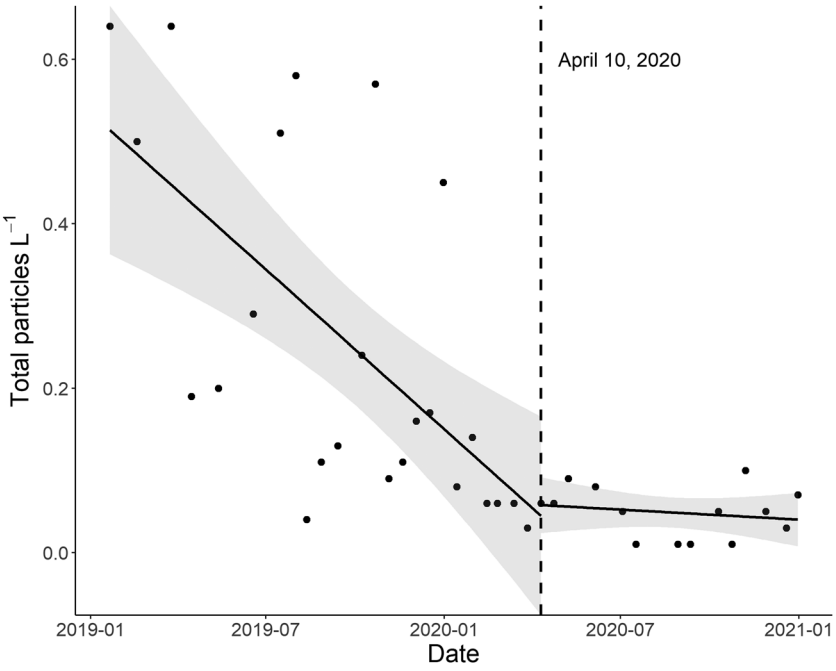

FIGURE 3: Total microparticle concentration across each water sampling event from January 2019 through December 2020. Dots show concentrations of each sample (microparticles L^{-1}) and solid lines represent the linear regressions of microparticle concentrations over time with the 95% confidence interval in gray. Dotted line denotes the breakpoint of 10 April 2020, where the linear regressions changed significantly ($p = 0.02$; pscore test).

due to stay-at-home orders (International Energy Agency, 2020; City Mapper).

Water sampling occurred roughly every 2 weeks but environmental and tourism sites did not share either the same locations or the same sampling time points. Therefore, the rolling 14-day average of precipitation, Duwamish River discharge, wastewater effluent, and tourism were calculated and used in analyses.

Environmental variables are often linked where an increase in precipitation causes river flow and wastewater effluent to increase as well. To take this into account, while also identifying effects of each environmental variable, samples were pooled annually into three seasons based on precipitation records and mixing events: winter (November–February), spring (March–June), and summer (July–October). In the Salish Sea region, winter is characterized by high precipitation (rain and snow), storm events, decreased seawater salinity, and high river flow and wastewater effluent; spring is characterized by snowpack melt, medium precipitation (rain), higher than average river flow and seawater mixing disrupting stratification; and summer is characterized by low precipitation (rain), increased seawater salinity and temperatures, and seawater stratification.

Analysis

All data analyses were completed using R (Ver 4.0.3, R Development Core Team, 2020). The following packages were used: data.table, car, dplyr, emmeans, faraway, ggplot2, lmerTest, MuMIn, nlme, patchwork, plyr, segmented, and zoo. Level of significance was set at $\alpha < 0.05$. Homogeneity of variance was confirmed with Bartlett's test and normal distribution with the Shapiro–Wilk test. Ambient microparticle concentrations between locations (clean room and laminar-flow hood) were compared using a *t* test.

A breakpoint and change in microparticle concentration over time were evaluated using change point estimation. Piecewise linear regression analysis was used to estimate the date where the breakpoint occurred. Differences in anthropogenic data (WWTP and tourism) were evaluated across the same dates pre-breakpoint and post-breakpoint using *t* tests. To evaluate the effects of environmental and tourism data on microparticle concentration over time, all possible linear mixed models were assessed, where precipitation, Duwamish River discharge, tourism, and wastewater effluent were fixed effects (interactions included), and the person counting microparticles was the random effect. Correlations between covariates were tested to avoid overfitting. Model selection occurred by calculating Akaike's information criterion $(AIC) = 2k - 2 \log L$, where k is the number of parameters and log L is the log likelihood for that model. However, because AIC tends to select more complex models, Bayesian information criterion (BIC) and AIC*c* with correction for small sample sizes were also calculated. After the best model was identified, model fit was evaluated and model diagnostics were checked.

Pooling total microparticle concentrations into annual seasons (seasons separated by year) allowed a broader examination of differences due to small-scale mechanisms common during specific times of year. Seasonal variation and an effect of the breakpoint on microparticle concentrations were assessed with linear mixed-effects models, with annual season and/or breakpoint as the fixed effects and the person counting microparticles as the random effect. Significant differences in annual seasons were assessed with paired contrasts using Bonferroni adjustment. A difference in morphotype

proportions and color proportions among annual seasons and the breakpoint were assessed using multivariate analyses of variance (MANOVAs). Significant differences in proportions were tested with analysis of variance (ANOVA) summaries. Effects of annual season and breakpoint (without an interaction) on fiber length were assessed using ANOVA. Ambient blank filters were included in the annual season analyses.

RESULTS

We collected 18 samples in 2019, 21 samples in 2020, and 27 ambient blank filters (15 ambient clean room and 12 ambient laminar-flow hood). Microparticles ranging from 0.00 to 0.64 microparticles L^{-1} were found in all but one (collected on 21 May 2020) water samples collected. Microparticles were not present in 48% of ambient blank filters, and those with microparticles ranged from 1 to 12 particles. Quantities of microparticles found on the two ambient blank location filters (clean room and laminar-flow hood) did not differ ($p = 0.47$; *t* test; see Supporting Information, Figure S1), which indicated that ambient microparticles remained consistent across processing locations and were therefore pooled in subsequent analyses and visualizations.

Microparticle concentration had a breakpoint on 10 April 2020, where estimated slope and associated microparticle concentration changed significantly ($p = 0.02$; pscore test; Figure 3). Pre-breakpoint had a significantly higher microparticle concentration than post-breakpoint ($p = 8 \times 10^{-5}$; *t* test; data not shown). Before 10 April 2020 (pre-breakpoint), total microparticle concentrations were high with an average of 0.24 ± 0.04 microparticle L^{-1} and decreased over time, whereas after the breakpoint (post-breakpoint), total microparticle concentrations remained consistently low with an average of 0.05 ± 0.01 microparticle L^{-1}, a decrease of 81% (Figure 3).

Microparticle concentration was best described by a mixed-effects model with tourism as the fixed effect and the person counting microparticles as the random effect (AIC*c* weight = 0.48; $p = 0.0004$; linear mixed-effects model; see Supporting Information, Table S1A). Four environmental and tourism factors were assessed for model selection and comparison, and the five best model fits can be found in Supporting Information, Table S1B. The 2 anthropogenic metrics included in model selection, WWTP effluent (a component of the total wastewater effluent) and tourism, were significantly different across the same date ranges pre-breakpoint and post-breakpoint ($p < 0.0001$ for both; *t* test; data not shown), where WWTP declined 7% and tourism declined 71% compared with pre-breakpoint averages.

Data were pooled into the three seasons of winter, spring, and summer to look at potential seasonality within and across years. Data were separated into annual seasons and

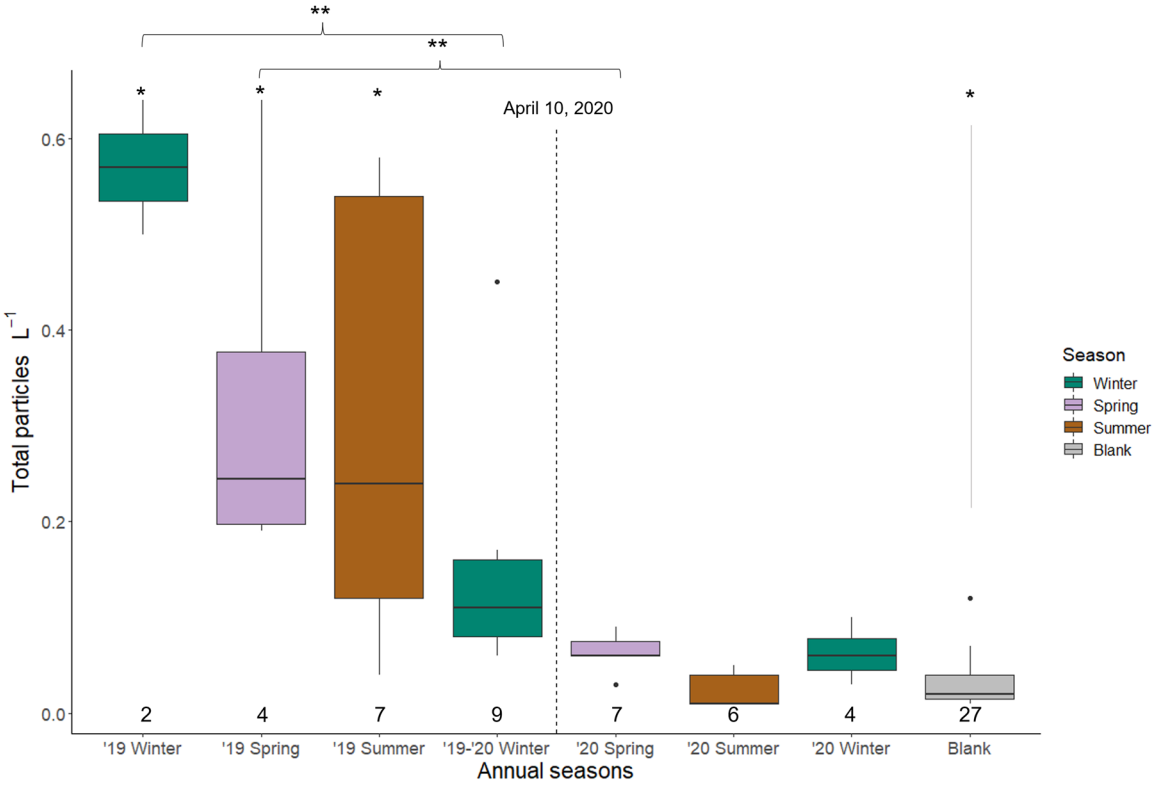

FIGURE 4: Microparticle concentrations across annual seasons, where green, purple, and brown colors represent winter, spring, and summer seasons, respectively. Gray shows ambient blanks. Boxes are upper and lower quartiles and dots denote outliers. Solid lines within boxes are median values. Asterisks above boxes denote statistical difference in microparticle concentrations. (*) indicates statistical difference from the ambient blank samples (gray box) and (**) indicate statistical difference in the annual seasons ($p < 0.05$; paired contrasts with Bonferroni test adjustment). The dashed line is the breakpoint (10 April 2020) where the trend in microparticle concentrations changed significantly. Numbers along the *x* axis represent sample size, or the number of filters included in each annual season.

TABLE 2: Summary of linear mixed-effects model analyses for seasonal microparticle concentrations (microparticles L^{-1}) reported as type III analysis of variance tables[a]

	Fixed effect	No. *DF*	Den *DF*	*F* value	*p* value[d]
(A)[b]	Annual seasons	7	55.26	15.44	<0.0001*
(B)[c]	Breakpoint	2	59.61	25.18	<0.0001*
	Season	2	59.40	0.19	0.82
	Breakpoint × Season	2	59.55	1.34	0.27

[a]Seven annual seasons were analyzed, and blanks were pooled and treated as a single annual season.
[b]Annual season as the fixed effect and the person counting microparticles as the random effect.
[c]Annual season and the breakpoint (pre-breakpoint and post-breakpoint, 10 April 2020) as the fixed effects (and their interaction) and the person counting microparticles as the random effect.
[d]*p* values were estimated through *t* tests using Satterthwaite's method.
*Significant at $p < 0.05$.
DEN = denominator.

TABLE 3: Summary of multivariate analyses of variance tables for annual seasons and the breakpoint (pre-breakpoint and post-breakpoint, 10 April 2020)

Dependent variable	Factor	*DF*	Pillai	*p* value
Morphology (A)[a]	Annual seasons	7	0.77	0.002*
	Breakpoint	2	0.11	0.46
Color (B)[b]	Annual seasons	7	1.17	<0.0001*
	Breakpoint	2	0.72	<0.0001*

[a]Proportions of microparticle morphologies.
[b]Proportions of microparticle colors.
*Significant at $p < 0.05$.
Pillai = Pillai's Trace test.

pre-breakpoint and post-breakpoint groups because the breakpoint analysis pointed toward a difference in microparticle concentrations (10 April 2020). Spring 2020 straddled the breakpoint, with the majority occurring post-breakpoint and was categorized as such. Total microparticle concentration was dependent on annual seasons and the breakpoint ($p = 0.0002$ and $p = 0.03$, respectively; 2-way ANOVA; Figure 4 and Table 2). All seasons in 2019 (pre-breakpoint) were different from the ambient blanks ($p < 0.01$; paired contrast with Bonferroni test adjustment; Figure 4).

Proportions of microparticle morphologies differed across annual seasons but not across the breakpoint ($p = 0.002$ and $p = 0.46$, respectively; MANOVA; Figure 5A and Table 3A). Specifically, only foil proportions differed across annual seasons ($p < 0.001$; MANOVA). Fibers were the dominant morphotype, where the proportion ranged from 95 to 100% of total microparticles counted in each sample. Fiber lengths did not differ either across annual seasons or the breakpoint; they averaged 657.09 ± 176.89 µm ($p = 0.38$ and $p = 0.53$, respectively; ANOVA; Figure 6 and Table 4). Proportions of microparticle colors varied across annual seasons and the breakpoint ($p < 0.001$ for both; MANOVA; Figure 5B and Table 4B). Proportions of blue, clear, and "other" colored microparticles changed across annual seasons ($p < 0.05$;

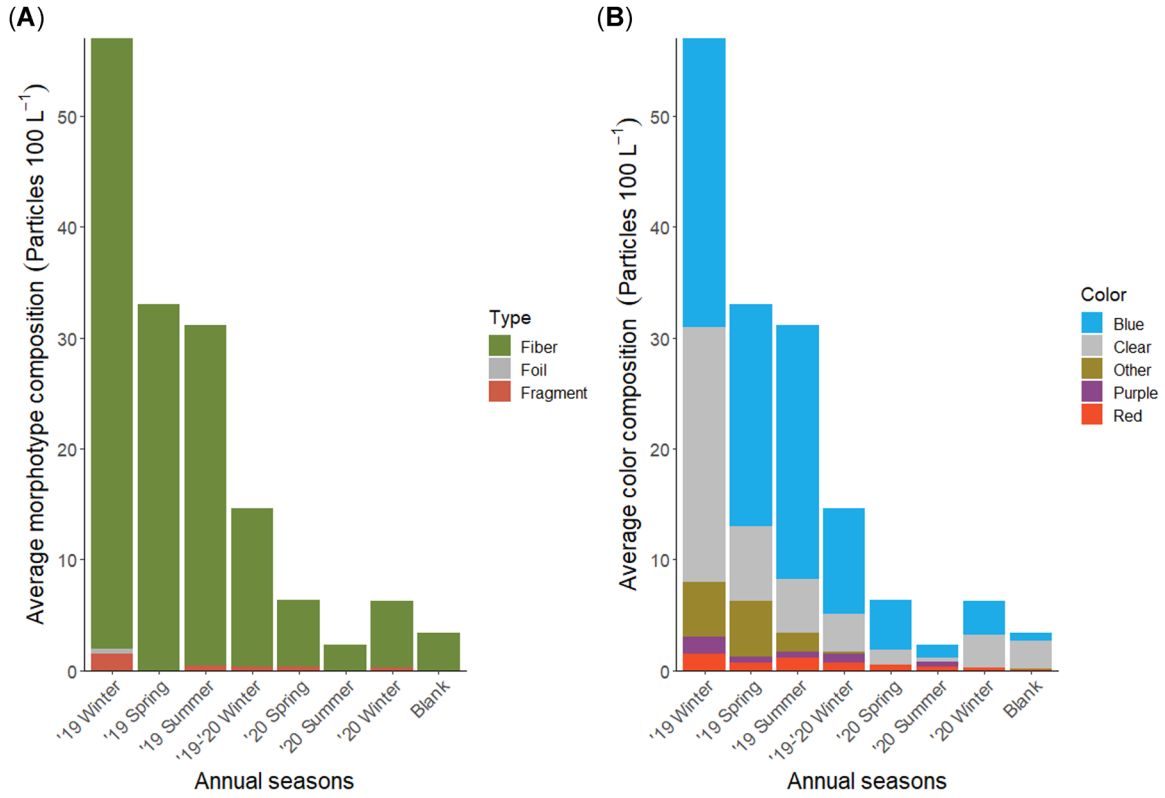

FIGURE 5: Bar charts depicting the average composition of (**A**) morphology, and (**B**) color in each 100-L water sample across annual seasons. Morphologies included fibers, foils, and fragments. Colors included blue, clear, "other" (colors were <1% of total particles), purple, and red.

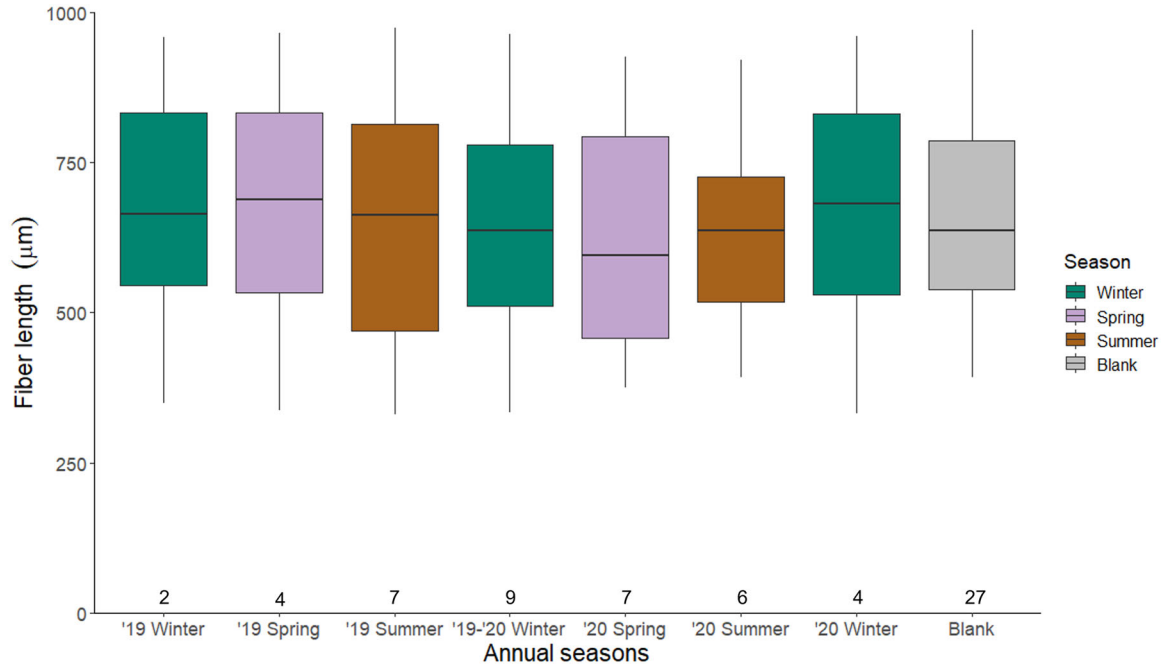

FIGURE 6: Fiber length across annual seasons with green, purple, and brown representing winter, spring, and summer seasons, respectively. Gray represents ambient blanks. Boxes are upper and lower quartiles and solid lines within boxes show median values. Numbers along the *x* axis denote sample size or the number of filters included in each annual season. There was no statistical difference in fiber length across annual seasons or when compared with the ambient blanks.

MANOVA), whereas only the proportions of blue and clear-colored microparticles changed pre-breakpoint to post-breakpoint ($p < 0.01$ for both; MANOVA). Blue and clear-colored microparticles accounted for 14 to 100% and 3 to 100% of total microparticles counted, respectively.

Microparticles chosen for µFTIR analysis came from water samples pre-breakpoint ($n = 61$) and post-breakpoint ($n = 7$) as well as ambient blank filters ($n = 8$). The majority of microparticles chosen for µFTIR analysis were fibers (96%) and were blue (44.7%) or clear (23.6%) in color. Polymer analysis with µFTIR provided reliable readings for 75 of the 76 chosen samples, where one sample was categorized as "anthropogenic unknown." All identified microparticles were either anthropogenic in material or processing, where microparticles that were categorized as processed, synthetic, or possibly natural/processed accounted for 80, 16, and 4% of the total microparticles analyzed, respectively (Figure 7). Processed microparticles included spectral identifications with cardboard or paper-cup cellulose and ethyl cellulose; synthetic microparticles were microplastics and included polyethylene terephthalate, polyester phthalate, polyamide, polyethylene and silicate, and polyester; possibly natural/processed included conflicting results of wool and polyamide (Supporting Information, Table S2). No unprocessed plant or biotic material was identified (e.g., algae, zooplankton, or hair). Complete spectral matching and categorization data can be found in Supporting Information, Table S2.

TABLE 4: Summary of analysis of variance table for microparticles fiber lengths, examined across factors of annual seasons and breakpoint[a]

Factor	*DF*	Sum sq.	Mean sq.	*F* value	*p* value
Annual seasons	7	167 776	33 555	1.07	0.38
Breakpoint	2	40 034	20 017	0.64	0.53
Residuals	703	22 007 477	31 305	—	—

[a]Pre-breakpoint and post-breakpoint, 10 April 2020. Factors were tested independently and their interaction was not tested.

DISCUSSION

The present study presents the first long-term monitoring of anthropogenic microparticle concentrations at depth in Elliott Bay in the Salish Sea, Washington, USA. Continuous and frequent sampling at the Seattle Aquarium over time allowed a unique opportunity to measure microparticle concentrations across multiple years and seasons, as well as through the beginning of the Covid-19 pandemic. Due to the duration of the present study, changing capacities and funding of our research program, and the evolving nature of microparticle sampling methodologies, our experimental protocols were updated as the present study progressed. While this led to methodological changes, we are confident the changes had no effect on results and interpretations, and we encourage other long-term studies to adjust methodologies as the field grows.

Findings in the present study provide additional context to previous microparticle studies conducted in the Salish Sea region. The present study observed 0.00 to 0.64 microparticles L^{-1} at approximately 9 m depth, where microparticle morphologies were predominately fibers, and concentrations as

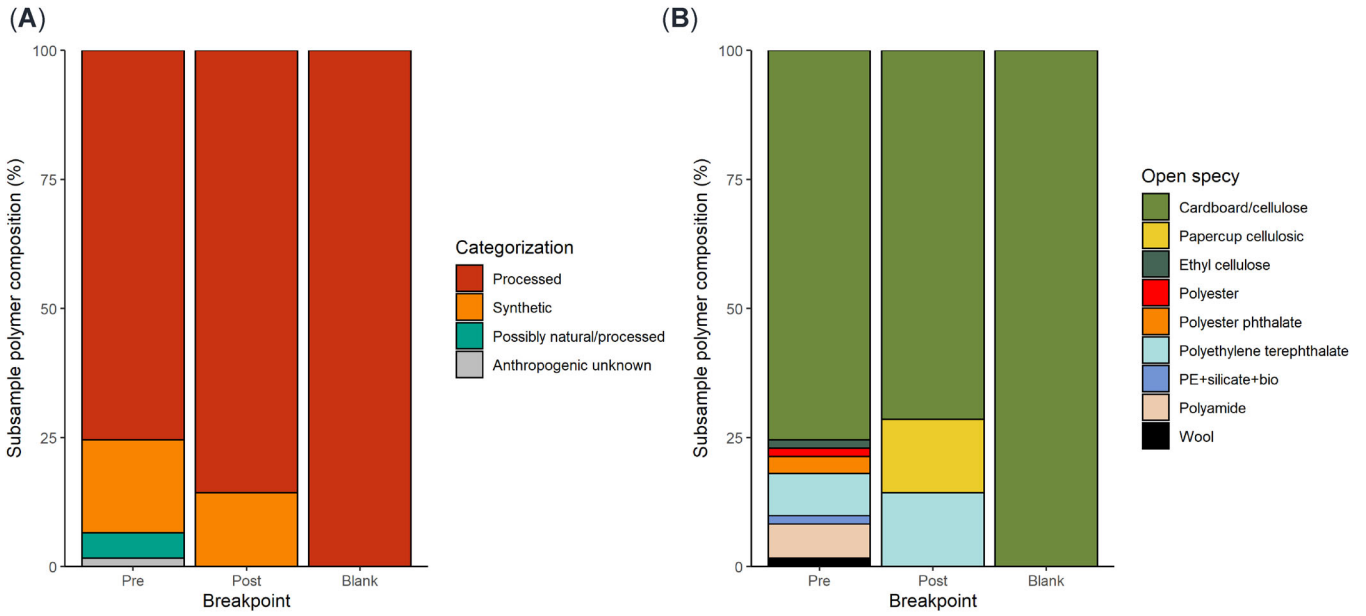

FIGURE 7: Polymer analysis using micro-Fourier transform infrared (μFTIR) on a subsample of microparticles (76) visually identified at the Seattle Aquarium (10% of the total particles in each breakpoint group). (**A**) Composition (%) of microparticle categorization based on the polymer spectra processed with Open Specy. Spectra were cross-validated with the Omnic library (Supporting Information, Table S2). Microparticles were separated by pre-breakpoint, post-breakpoint, and blanks; bottom numbers represent the number of particles tested. (**B**) Polymer composition (%) of microparticles using the Open Specy library, an open-source spectra library (Cowger et al., 2021), where the majority of microparticles identified were cardboard/cellulose (shown as green on the figure). PE = polyethylene.

well as morphologies were consistent with other regional studies (Davis & Murphy, 2015; Desforges et al., 2014; Martinelli et al., 2020). Previous sea surface tows observed microparticle concentrations of 0.00 to 0.2 microparticles L^{-1} in the Salish Sea (extrapolated from Davis & Murphy, 2015) and 0.007 to 3.8 microparticles L^{-1} in the Strait of Georgia (between Vancouver Island and the British Columbia mainland, with the Canada–US border running to its south; Desforges et al., 2014) with microparticle morphologies predominantly foam and fiber (Desforges et al., 2014; Davis & Murphy, 2015). Further, the average fiber length of 657.09 ± 176.89 μm observed in the present study was consistent with previously observed fiber lengths of 606 ± 221 μm in the region (Desforges et al., 2014). In biota, a recent analysis of razor clams sampled along remote portions of the Washington state coastline also found that 99% of microparticles were fibers, with a combination of polyethylene terephthalate, polyester, nylon, cellulose acetate, and cellulose identified via FTIR (Baechler et al., 2020). These studies are consistent with others and provide additional evidence of the ubiquitous environmental distribution of fibers, most likely generated from laundering of clothing (e.g., Cesa et al., 2017; Gago et al., 2018; Ross et al., 2021).

All microparticles included in polymer analysis were confirmed to be anthropogenic in either origin or processing (Figure 7 and Supporting Information, Table S2). Processed microparticles accounted for 80% of the subsample analyzed and included non-synthetic material (e.g., forms of cellulose that originated from a plant; Miller et al., 2021) that had been isolated and had undergone human processing including the addition of additives or dyes. Examples of cellulose categorized as processed include paper products (e.g., plastic-lined cups) or plant-based fabrics (e.g., linen, wool, and cotton). Conversely, naturally occurring plant (e.g., wood, grass, or algae) or animal (e.g., fur or hair) particles are chemically different from anthropogenically processed particles of the same origin and match with natural spectra. Synthetic microparticles, definitively microplastic, accounted for 16% of the subsample analyzed, and although the polymer types identified in the present study differ somewhat from what others have reported in coastal waters off the West Coast of North America (Kashiwabara et al., 2021; Sutton et al., 2016), fibers were the majority morphotype found across studies. Microparticles categorized as possibly natural/processed accounted for 4% of the subsample analyzed and were keratin-based fibers, possibly from wool, cashmere, alpaca (Granek et al., 2021), or marine mammals. Due to the inconclusive types, sources, and potential processing, we were unable to definitively determine the exact nature of these microparticles.

Physical characteristics of microplastics are known to dictate fate and transportation in marine systems (Zhang, 2017). Examining the material properties of microparticles found in pelagic water samples may offer an explanation on the difference in microparticle concentrations (morphotype, polymer type, and quantities) across the breakpoint as well as compared with other studies. Sea surface samples capture lighter, more buoyant particles that have not necessarily been in the water very long and thus may not interact with pelagic or benthic marine organisms but may be washed up on beaches. Low-density synthetic particles found in pelagic waters (e.g., polyethylene and polyamide) suggest that particles were biofouled, causing an increase in density, bypassing surface waters, and sinking toward the sediment. Morét-Ferguson et al. (2010)

found that low-density polymers such as polyethylene were found on beaches with higher densities than pristine counterparts; they concluded that the increase in density resulted from biofouling at sea. There is still little research on the mechanisms of biofouling and how that contributes to the distribution of microplastics in the water column.

Sampling at depth captures particles that sink due to high density, wave action, currents, or biofouling, all on their way to benthic sediments or to be ingested by organisms. The present study provides a glance at microparticles that are available to pelagic and benthic organisms in the Salish Sea. In the Puget Sound, 63% of oysters, which are proficient suspension feeders, have been found to contain microparticles (Martinelli et al., 2020). While concentrations were found to be relatively low, approximately 1.75 microparticles oyster^{-1}, the results were consistent with the present study where the predominant morphology was fibers (Martinelli et al., 2020). Using concentrations found in the present study, 0 to 0.64 microparticles L^{-1}, oysters need to filter and process less than 3 L to achieve the average concentrations found in Martinelli et al. (2020), well below their daily filtering capacity (native Olympia oysters, *Ostrea lurida*, filter 2.4 L h^{-1}; Zu Ermgassen et al., 2013). Oyster habitat and feeding mechanics offer two possible explanations for relatively high microparticle concentrations in water when compared with oysters. First, the present study measured microparticles in the water column, whereas oysters typically inhabit and feed near benthic sediment. While sediment is thought to be the eventual resting place for the majority of microparticles (Woodall et al., 2014; Zhang, 2017; Choy et al., 2019) and contains relatively high concentrations of microparticles, it is possible that the waters just above the sediment, the boundary layer and where oysters feed, contain fewer microparticles. Second, oysters are suspension feeders, able to select and remove up to 50% of particles (Ward & Shumway, 2004). Low incidence of microparticles in oysters relative to the water column may be due to selection against microparticles and may not be representative of environmental contamination levels.

Over the course of this 2-year study (2019–2020) a drastic decrease in microparticle concentrations occurred on 10 April 2020 and was identified as a breakpoint separating two distinct temporal periods of microparticle concentrations. Total particle concentration, morphology, and color are dependent on seasonality, when not considering the breakpoint. A different trend emerges, however, taking the breakpoint into consideration. Pre-breakpoint samples consisted of high and variable microparticle concentrations (when compared with post-breakpoint samples) where all morphologies and colors observed were present. Further, all pre-breakpoint 2019 microparticle concentrations (grouped by annual season) were significantly higher than ambient blank samples, which substantiates the presence of microparticles in the water column. Conversely, post-breakpoint samples consisted of low and consistent microparticle concentrations (compared with the pre-breakpoint samples) where little variation in morphology and color were present. None of the post-breakpoint microparticle concentrations (grouped by annual season) differed from ambient blank samples, which suggests that measured microparticle concentrations did not differ from background or contamination concentrations.

Comparing environmental and tourism data, the observed change in microparticle concentrations was found to be correlated with a decrease in tourism (Transportation Security Administration screened) occurring at the onset of the global Covid-19 pandemic. During the onset of the Covid-19 pandemic, there was a drastic shift in work from home policies and a reduction of human activity in Seattle (International Energy Agency, 2020; City Mapper App.), both of which may be causes for the noticeable decline in microparticle concentration and the statistical breakpoint. The present study found a significant breakpoint in the concentrations of microparticles that coincided with the onset of Covid-19, the shut-down of Seattle, and the decline in air travel; this indicates that although individuals may have returned to car travel at a faster rate, the immediate (lag time of 2 weeks) decrease of tourism on marine microparticle pollution was evident. Sampling at depth is likely responsible for the 2-week lag time observed between the decrease in tourism and decrease in microparticle concentrations. These 2 weeks allowed for microparticles to sink from the surface (the interface between human activity and water) due to variables such as currents, wave action, and/or biofouling.

Model selection indicated that human activity (from tourism, intracity travel, and/or visiting the waterfront) led to lower rates of microparticle pollution in Elliott Bay. Although the present study did not measure all types of microparticle pollution (e.g., tire abrasion and wear estimated globally at 1.4 million tons, road marking wear at 0.6 million tons, city dust at 0.5 million tons, and washing of textiles at 0.2 million tons; Ryberg et al., 2019), it did include two metrics of anthropogenic activity—WWTP effluent and tourism. Volume of WWTP effluent measures the quantity of water used by people (e.g., toilet, bathtub, and washing machine) and may be an indicator of human activity, quantity of people residing in an area, and/or volume of textile washing. There were significant declines in both anthropogenic metrics across the same dates pre-breakpoint and post-breakpoint, where WWTP effluent and tourism decreased 7 and 71% in post-breakpoint averages, respectively. These two metrics are not necessarily independent of each other; tourism contributes to the amount of anthropogenic waste in a region while WWTP, combined sewage overflow, urban runoff from rain, and river flow all carry high quantities of microparticles, specifically fibers, into waterways (Skalska et al., 2020). While WWTP effluent contributes high quantities of fibers, the 7% volumetric decrease observed in the Salish Sea region after the onset of Covid-19 does not account for the much larger decline (81%) in microparticle concentrations observed during the same period.

An effect of tourism and subsequent declines in waterfront activity were found and it is important to examine the nuances among types of microparticles observed and tourism. There were more identified polymer types in pre-breakpoint (eight types) than in post-breakpoint (three types) microparticle samples when matched in the Open Specy database (Figure 7B). In combination, the decline in microparticle

concentration, polymer types, and color range, yet a relatively consistent proportion of morphologies and length of fibers in post-breakpoint samples suggests a decrease in quantity as well as a change in the microparticle source. Decreased tourism leads to a smaller urban population, which can have cascading effects on human movement and WWTP effluent, as well as on waterfront activity. All these anthropogenic factors can affect both the concentration as well as composition of microparticle pollution in Elliott Bay, further supporting an effect of Covid-19 and the subsequent decline of tourism on microparticle concentration and source.

Decline in tourism and activity on the waterfront decreased the quantity of microparticles observed; however, the long-term Covid-19 effects on marine debris remain unknown. The microparticles found in the present study were primarily fibers and likely not from single-use plastics but rather from textile washing and shedding. While the quantity of microparticles found in the present study decreased with the onset of Covid-19 and stay-at-home orders, global single-use plastic consumption and subsequent pollution increased substantially (Prata et al., 2020; Benson et al., 2021). When plastic enters waterways, it is degraded by ultraviolet rays and broken apart by physical forces such as wave action over time. Because single-use plastic consumption remains high throughout the pandemic and the foreseeable future, it is possible that as these plastics break apart they will begin to appear in future water samples. Microparticle contamination is relatively low and mostly consists of fibers as of 2020; future conditions are likely to worsen due to current consumption and waste of single-use plastics and the eventual return of tourism.

Seasonality of microparticle concentrations may exist; however, with the significance of the breakpoint and the lack of supportive evidence from the environmental data, it is too early to tell definitively. In the Salish Sea region (and specifically in Seattle) tourism typically peaks in the summer, whereas all environmental variables included in the present study (precipitation, Duwamish River discharge, and wastewater effluent) peak in the winter. Monitoring efforts in the present study set out to identify effects of seasonality and interannual differences in microparticle concentrations; instead it captured an effect of decreased tourism due to the global Covid-19 pandemic. Previous studies in the Salish Sea region have sampled only surface level concentrations; therefore, the present study is the first research describing long-term microparticle concentrations at depth in the Salish Sea. Effects of environmental variables and seasonality were not detected from 2019 through 2020; however, they may still exist given the possibility that an effect of tourism overshadowed them.

Tourism in Seattle remained low through 2020 and has yet to recover to pre-pandemic levels. As it does, it is important to continue monitoring marine microparticles at depth to understand long-term environmental cycling, tourism, and Covid-19 related effects. Additional locations upriver and across the Salish Sea, as well as additional environmental variables such as wind direction and strength, should be investigated to create a larger framework of spatial microparticle concentrations. Understanding how microparticle presence is influenced by seasonality and both global and regional events can provide information to managers on when to focus resources on mitigation and clean-up strategies. The Seattle Aquarium remains committed to continue its long-term monitoring of microparticle concentrations in the Salish Sea.

Supporting Information—The Supporting Information is available on the Wiley Online Library at https://doi.org/10.1002/etc.5190.

Acknowledgment—The present study was made possible through generous contributions by an anonymous donor to the Seattle Aquarium and its microplastics research program; we are grateful for their support and dedication to our mission. In addition, our research was supported by funding from PCC Community Markets and the Sea Otter Foundation and Trust. We thank the many volunteers who made this study possible, collecting and processing seawater samples for more than 2 years: R. Banados, J. Duprey, A. Lind, and M. Williams. We are grateful to C.J. Casson and E. Meyer for their ongoing support.

Author Contributions Statement—L. Harris: formal analysis, investigation, resources, data curation, writing–original draft, writing–review and editing, visualization, and supervision. L. La Beur: methodology, investigation, resources, writing–original draft, writing–review and editing. A. Olsen: conceptualization, methodology, formal analysis, investigation, writing–original draft, writing–review and editing. A. Smith: conceptualization, methodology, resources, writing–review and editing. L. Damazo: methodology, investigation, writing–original draft, writing–review and editing. E. Pedersen: methodology, formal analysis, writing–review and editing. J. Van Brocklin: methodology, writing–review and editing. S.M. Brander: methodology, resources, writing–review and editing. S. Larson: conceptualization, methodology, investigation, resources, writing–review and editing, supervision, and funding acquisition.

Data Availability Statement—Data and associated metadata pertaining to the present study will be deposited in Dryad (https://doi.org/10.5061/dryad.zpc866t90). Data, associated metadata, and calculation tools are also available from the corresponding author (lydaharris@gmail.com).

REFERENCES

Arthur, C., Baker, J., & Bamford, H. (2009). *Proceedings of the International Research Workshop on the occurrence, effects, and fate of microplastic marine debris*. National Oceanic and Atmospheric technical memorandum NOS-OR&R-30.

Baechler, B. R., Granek, E. F., Mazzone, S. J., Nielsen-Pincus, M., & Brander, S. M. (2020). Microplastic exposure by razor clam recreational Harvester-consumers along a sparsely populated coastline. *Frontiers in Marine Science*, *7*, 980.

Barboza, L. G. A., & Gimenez, B. C. G. (2015). Microplastics in the marine environment: Current trends and future perspectives. *Marine Pollution Bulletin*, *97*(1), 5–12.

Barnes, D. K. A., Galgani, F., Thompson, R. C., & Barlaz, M. (2009). Accumulation and fragmentation of plastic debris in global

environments. *Philosophical Transactions: Biological Sciences*, *364*(1526), 1985–1998.

Barrows, A. P. W., Cathey, S. E., & Petersen, C. W. (2018). Marine environment microfiber contamination: Global patterns and the diversity of microparticle origins. *Environmental Pollution*, *237*, 275–284.

Benson, N. U., Bassey, D. E., & Palanisami, T. (2021). COVID pollution: Impact of COVID-19 pandemic on global plastic waste footprint. *Heliyon*, *7*(2), Article e06343.

Browne, M. A., Crump, P., Niven, S. J., Teuten, E., Tonkin, A., Galloway, T., & Thompson, R. (2011). Accumulation of microplastic on shorelines worldwide: Sources and sinks. *Environmental Science & Technology*, *45*(21), 9175–9179.

Browne, M. A., Galloway, T. S., & Thompson, R. C. (2010). Spatial patterns of plastic debris along estuarine shorelines. *Environmental Science & Technology*, *44*(9), 3404–3409.

Cesa, F. S., Turra, A., & Baroque-Ramos, J. (2017). Synthetic fibers as microplastics in the marine environment: A review from textile perspective with a focus on domestic washings. *Science of the Total Environment*, *598*, 1116–1129.

Cheung, P. K., Cheung, L. T. O., & Fok, L. (2016). Seasonal variation in the abundance of marine plastic debris in the estuary of a subtropical macro-scale drainage basin in South China. *Science of the Total Environment*, *562*, 658–665.

Choy, C. A., Robison, B. H., Gagne, T. O., Erwin, B., Firl, E., Halden, R. U., Hamilton, J. A., Katija, K., Lisin, S. E., Rolsky, C., & Houtan, K. S. V. (2019). The vertical distribution and biological transport of marine microplastics across the epipelagic and mesopelagic water column. *Scientific Reports*, *9*(1), Article 7843.

City Mapper App. Seattle, WA, USA. https://citymapper.com/cmi/seattle

Cowger, W., Steinmetz, Z., Gray, A., Munno, K., Lynch, J., Hapich, H., Primpke, S., De Frond, H., Rochman, C., & Herodotou, O. (2021). Microplastic spectral classification needs an open source community: Open specy to the rescue! *Analytical Chemistry*, *93*(21), 7543–7548.

Crichton, E. M., Noël, M., Gies, E. A., & Ross, P. S. (2017). A novel, density-independent and FTIR-compatible approach for the rapid extraction of microplastics from aquatic sediments. *Analytical Methods*, *9*(9), 1419–1428.

Critchell, K., & Lambrechts, J. (2016). Modelling accumulation of marine plastics in the coastal zone: What are the dominant physical processes? *Estuarine, Coastal and Shelf Science*, *171*, 111–122.

Davis, W., III, & Murphy, A. G. (2015). Plastic in surface waters of the Inside Passage and beaches of the Salish Sea in Washington State. *Marine Pollution Bulletin*, *97*(1–2), 169–177

Desforges, J.-P. W., Galbraith, M., Dangerfield, N., & Ross, P. S. (2014). Widespread distribution of microplastics in subsurface seawater in the NE Pacific Ocean. *Marine Pollution Bulletin*, *79*(1–2), 94–99.

Enders, K., Lenz, R., Stedmon, C. A., & Nielsen, T. G. (2015). Abundance, size and polymer composition of marine microplastics ≥10 μm in the Atlantic Ocean and their modelled vertical distribution. *Marine Pollution Bulletin*, *100*(1), 70–81.

Gago, J., Carretero, O., Filgueiras, A. V., & Viñas, L. (2018). Synthetic microfibers in the marine environment: A review on their occurrence in seawater and sediments. *Marine Pollution Bulletin*, *127*, 365–376.

Galgani, F., Hanke, G., & Maes, T. (2015). Global distribution, composition and abundance of marine litter. In M. Bergmann, L. Gutow, & M. Klages (Eds.), *Marine anthropogenic litter* (pp. 29–56). Springer International Publishing.

Galloway, T. S., Cole, M., & Lewis, C. (2017). Interactions of microplastic debris throughout the marine ecosystem. *Nature Ecology & Evolution*, *1*(5), Article 0116.

Gilman, N. (2013). Examining spatial concentrations of marine micro-plastics on shorelines in South Puget Sound, Washington. (Master's thesis, The Evergreen State College, Olympia, Washington). https://archives.evergreen.edu/masterstheses/Accession86-10MES/Gilman_N2013.pdf

Granek, E. F., Brander, S. M., & Holland, E. B. (2020). Microplastics in aquatic organisms: Improving understanding and identifying research directions for the next decade. *Limnology and Oceanography Letters*. https://doi.org/10.1002/lol2.10145

Hansen, L. (2016). *Macro and micro plastics in an urbanized and non-urbanized fjord estuary in the Northeast Pacific Ocean* [Senior thesis, University of Washington]. http://hdl.handle.net/1773/36335

Harris, L. S. T. (2020). *Marine microplastic pollution: An interdisciplinary approach to understanding the effects on organisms, ecosystems, and policy* [Doctoral dissertation, University of Washington]. http://hdl.handle.net/1773/46738

Harris, L. S. T., & Carrington, E. (2019). Impacts of microplastic vs. natural abiotic particles on the clearance rate of a marine mussel. *Limnology and Oceanography Letters*. https://doi.org/10.1002/lol2.10120

Harris, L. S. T., Gill, H., & Carrington, E. (2021). Microplastic changes the sinking and resuspension rates of marine mussel biodeposits. *Marine Pollution Bulletin*, *165*, Article 112165.

Hartmann, N. B., Hüffer, T., Thompson, R. C., Hassellöv, M., Verschoor, A., Daugaard, A. E., Rist, S., Karlsson, T., Brennholt, N., Cole, M., Herrling, M. P., Hess, M. C., Ivleva, N. P., Lusher, A. L., & Wagner, M. (2019). Are we speaking the same language? Recommendations for a definition and categorization framework for plastic debris. *Environmental Science & Technology*, *53*(3), 1039–1047.

Hofmans, G. (2017). *The quantification of microplastics along a primary Puget Sound river* [Senior thesis, University of Washington]. http://hdl.handle.net/1773/39725

International Energy Agency. (2020). Changes in transport behavior during the Covid-19 crisis. https://www.iea.org/articles/changes-in-transport-behaviour-during-the-covid-19-crisis

Ivar do Sul, J. A., & Costa, M. F. (2014). The present and future of microplastic pollution in the marine environment. *Environmental Pollution*, *185*, 352–364.

Kashiwabara, L. M., Kahane-Rapport, S. R., King, C., DeVogelaere, M., Goldbogen, J. A., & Savoca, M. S. (2021). Microplastics and microfibers in surface waters of Monterey Bay National Marine Sanctuary, California. *Marine Pollution Bulletin*, *165*, Article 112148.

Law, K. L. (2017). Plastics in the marine environment. *Annual Review of Marine Science*, *9*(1), 205–229.

Li, J., Yang, D., Li, L., Jabeen, K., & Shi, H. (2015). Microplastics in commercial bivalves from China. *Environmental Pollution*, *207*, 190–195.

Lima, A. R. A., Costa, M. F., & Barletta, M. (2014). Distribution patterns of microplastics within the plankton of a tropical estuary. *Environmental Research*, *132*, 146–155.

Lusher, A. L., Burke, A., O'Connor, I., & Officer, R. (2014). Microplastic pollution in the Northeast Atlantic Ocean: Validated and opportunistic sampling. *Marine Pollution Bulletin*, *88*(1–2), 325–333.

Mahoney, T. (2017). *The concentration of microplastics compared to relative population proximity and basin residence times in Hood Canal and Whidbey Basin in Puget Sound, WA* [Senior thesis, University of Washington]. http://hdl.handle.net/1773/39739

Martinelli, J. C., Phan, S., Luscombe, C. K., & Padilla-Gamiño, J. L. (2020). Low incidence of microplastic contaminants in Pacific oysters (Crassostrea gigas Thunberg) from the Salish Sea, USA. *Science of the Total Environment*, *715*, Article 136826.

Masura, J., Baker, J., Foster, G., & Arthur, C. (2015). Laboratory methods for the analysis of microplastics in the marine environment: Recommendations for quantifying synthetic particles in waters and sediments. National Oceanic and Atmospheric technical memorandum NOS-OR&R-48.

Miller, E., Sedlak, M., Lin, D., Box, C., Holleman, C., Rochman, C. M., & Sutton, R. (2021). Recommended best practices for collecting, analyzing, and reporting microplastics in environmental media: Lessons learned from comprehensive monitoring of San Francisco Bay. *Journal of Hazardous Materials, 409*, 124770. https://doi.org/10.1016/j.jhazmat.2020.124770

Moats, J. (2019). *Vertical distribution of microplastics* [Senior thesis, University of Washington]. http://hdl.handle.net/1773/45627

Morét-Ferguson, S., Law, K. L., Proskurowski, G., Murphy, E. K., Peacock, E. E., & Reddy, C. M. (2010). The size, mass, and composition of plastic debris in the Western North Atlantic Ocean. *Marine Pollution Bulletin*, *60*(10), 1873–1878.

National Centers for Environmental Information at National Oceanic and Atmospheric Administration. (2021). Daily summaries station details. https://www.ncdc.noaa.gov/cdo-web/datasets/GHCND/stations/GHCND:USW00024233/detail

National Oceanic and Atmospheric Administration tide predictions. (2021). Annual prediction tide tables for Seattle, WA (9447130). https://tidesandcurrents.noaa.gov/

Pacific Northwest Microplastics Workshop. (12 May 2021). Virtual. Seattle Aquarium, Seattle, WA, USA.

Pagter, E., Frias, J., Kavanagh, F., & Nash, R. (2020). Varying levels of microplastics in benthic sediments within a shallow coastal embayment. *Estuarine, Coastal and Shelf Science*, *243*, Article 106915.

Prata, J. C., Silva, A. L. P., Walker, T. R., Duarte, A. C., & Rocha-Santos, T. (2020). COVID-19 pandemic repercussions on the use and management of plastics. *Environmental Science & Technology*, *54*(13), 7760–7765.

Ross, P. S., Chastain, S., Vassilenko, E., Etemadifar, A., Zimmermann, S., Quesnel, S.-A., Eert, J., Solomon, E., Patankar, S., Posacka, A. M., & Williams, B. (2021). Pervasive distribution of polyester fibres in the Arctic Ocean is driven by Atlantic inputs. *Nature Communications, 12*(1). https://doi.org/10.1038/s41467-020-20347-1

Ryberg, M. W., Hauschild, M. Z., Wang, F., Averous-Monnery, S., & Laurent, A. (2019). Global environmental losses of plastics across their value chains. *Resources, Conservation & Recycling*, *151*, Article 104459.

van Sebille, E., Aliani, S., Law, K. L., Maximenko, N., Alsina, J. M., Bagaev, A., Bergmann, M., Chapron, B., Chubarenko, I., Cózar, A., Delandmeter, P., Egger, M., Fox-Kemper, B., Garaba, S. P., Goddijn-Murphy, L., Hardesty, B. D., Hoffman, M. J., Isobe, A., Jongedijk, C. E., & Wichmann, D. (2020). The physical oceanography of the transport of floating marine debris. *Environmental Research Letters*, *15*(2), Article 023003.

Serdan, M. (2017). *Microplastic abundance throughout Puget Sound* [Senior thesis, University of Washington]. http://hdl.handle.net/1773/43199

Skalska, K., Ockelford, A., Ebdon, J. E., & Cundy, A. B. (2020). Riverine microplastics: Behaviour, spatio-temporal variability, and recommendations for standardised sampling and monitoring. *Journal of Water Process Engineering*, *38*, Article 101600.

Sutton, R., Mason, S. A., Stanek, S. K., Willis-Norton, E., Wren, I. F., & Box, C. (2016). Microplastic contamination in the San Francisco Bay, California, USA. *Marine Pollution Bulletin*, *109*(1), 230–235. https://doi.org/10.1016/j.marpolbul.2016.05.077

Thompson, R. C., Olsen, Y., Mitchell, R. P., Davis, A., Rowland, S. J., John, A. W. G., McGonigle, D., & Russell, A. E. (2004). Lost at sea: Where is all the plastic? *Science*, *304*(5672), 838.

Transportation Security Administration. (2021). TSA checkpoint travel numbers. https://www.tsa.gov/coronavirus/passenger-throughput?page=1

Uncles, R. J., Bloomer, N. J., Frickers, P. E., Griffiths, M. L., Harris, C., Howland, R. J., Morris, A. W., Plummer, D. H., & Tappin, A. D. (2000). Seasonal variability of salinity, temperature, turbidity and suspended chlorophyll in the Tweed Estuary. *Science of the Total Environment*, *251–252*, 115–124.

US Geological Survey Water Resources. (2021). Duwamish River (site number 12113390) at golf course at Tukwila, Washington, USA. https://waterdata.usgs.gov/usa/nwis/uv?12113390

Van Emmerik, T., Tramoy, R., Van Calcar, C., Alligant, S., Treilles, R., Tassin, B., & Gasperi, J. (2019). Seine plastic debris transport tenfolded during increased river discharge. *Frontiers in Marine Science*, 6. https://doi.org/10.3389/fmars.2019.00642

Ward, E., & Shumway, S. (2004). Separating the grain from the chaff: Particle selection in suspension- and deposit-feeding bivalves. *Journal of Experimental Marine Biology and Ecology*, *300*(1–2), 83–130.

Wichmann, D., Delandmeter, P., & Van Sebille, E. (2019). Influence of near-surface currents on the global dispersal of marine microplastic. *Journal of Geophysical Research: Oceans*, *124*(8), 6086–6096.

Woodall, L. C., Sanchez-Vidal, A., Canals, M., Paterson, G. L. J., Coppock, R., Sleight, V., Calafat, A., Rogers, A. D., Narayanaswamy, B. E., & Thompson, R. C. (2014). The deep sea is a major sink for microplastic debris. *Royal Society Open Science*, *1*(4), Article 140317.

Wright, S. L., Thompson, R. C., & Galloway, T. S. (2013). The physical impacts of microplastics on marine organisms: A review. *Environmental Pollution*, *178*, 483–492.

Zhang, H. (2017). Transport of microplastics in coastal seas. *Estuarine, Coastal and Shelf Science*, *199*, 74–86.

Zhang, T., Sun, Y., Song, K., Du, W., Huang, W., Gu, Z., & Feng, Z. (2021). Microplastics in different tissues of wild crabs at three important fishing grounds in China. *Chemosphere*, *271*, Article 129479.

Zu Ermgassen, P. S. E., Gray, M. W., Langdon, C. J., Spalding, M. D., & Brumbaugh, R. D. (2013). Quantifying the historic contribution of Olympia oysters to filtration in Pacific Coast (USA) estuaries and the implications for restoration objectives. *Aquatic Ecology*, *47*(2), 149–161.

